



# Morphological observation and CBCT of the bony canal structure of the groove and the location of blood vessels and nerves in the palatine of elderly human cadavers

Yoko Miwa<sup>1</sup> · Rieko Asaumi<sup>2</sup> · Taisuke Kawai<sup>2</sup> · Yuuki Maeda<sup>1</sup> · Iwao Sato<sup>1</sup> 

Received: 4 October 2017 / Accepted: 27 November 2017 / Published online: 4 December 2017  
© Springer-Verlag France SAS, part of Springer Nature 2017

## Abstract

**Purpose** The greater and lesser palatine nerves and vessels supply the hard and soft palates, and the roots of these vessels and nerves run through a bony structure. However, the arrangement of blood vessels in the maxilla requires attention during clinical treatments, but detailed morphological information about changes in the greater and lesser palatine arteries and nerves during aging is unavailable. We therefore need detailed investigations of the morphology of the donor cadaver palatine using cone-beam computed tomography (CBCT) and macroscopic observations.

**Methods** We investigated 72 donor cadavers using macroscopic segmentation and CBCT. The results' analysis examined differences in skull measurement parameters and differences between dentate and edentulous cases.

**Results** The greater palatine artery and nerve showed different macroscopic arrangements in dentate and edentulous cadavers. We also classified three types of bony structures of the nerve and vessel roots in the molar regions of the palatine using CBCT images: the shallow groove, deep groove, and flat groove. The deep groove is the deepest of the three and is remarkable in edentulous elderly cadavers.

**Conclusion** This study of macroscopic and CBCT data provides information useful for planning dental implant surgeries and autogenous bone harvesting.

**Keywords** Palatine · CBCT · Greater palatine nerve · Greater palatine artery · Palatal donor tissue · Greater palatine foramen

## Introduction

The hard palate is composed of the maxillae and the palatine bones and extends anteriorly from the greater palatine canal, which is formed by the border of the two bones. Previous reports indicated the anatomic location of the greater palatine foramen and lesser palatine foramen [6, 8, 19, 24]. The greater palatine nerve and vessels supply the hard palate; the roots of these vessels and the nerve run through a bony structure, such as a groove, for the greater palatine vessels

[1, 11, 12, 21], the sulci palatine and palatine spine [14], and the palatine grooves [16, 23]. However, the arrangement of the blood vessels of the maxilla is specific and requires attention during clinical treatments [3, 10, 25]. In general, the detailed distribution of blood vessels is needed to avoid infection in the pedicle formed during autogenous bone harvesting. During post-processing, artificial bone is used for bone grafts in the chin and face in dental implant treatments. In contrast, it is morphologically important for the infra-orbital artery and posterior superior alveolar artery in the maxillary sinus to be lifted in an edentulous upper jaw [18]. Morphologically, there is an intraosseous lateral branch of the inferior alveolar artery in the lower jaw. Various examinations have been conducted to investigate autogenous bone harvesting, but determining the presence of intraosseous blood vessels and nerves in the maxilla is of highest importance [13, 15, 20]. Cone-beam computed tomography (CBCT) has provided morphological information for nerve block anesthesia, dental implant surgery and autogenous

✉ Iwao Sato  
iwaoa1@tokyo.ndu.ac.jp

<sup>1</sup> Department of Anatomy, School of Life Dentistry at Tokyo, The Nippon Dental University, 1-9-20 Fujimi, Chiyoda-ku, Tokyo 102-8159, Japan

<sup>2</sup> Department of Oral and Maxillofacial Radiology, School of Life Dentistry at Tokyo, The Nippon Dental University, Tokyo, Japan

bone harvesting in dentate patients [4, 7, 8]. More information regarding the morphological features of the upper jaw is needed. The structural features of the human hard palate, which is composed of the maxillae and the palatine bones, may alter the distribution of blood vessels and nerves in elderly patients. Moreover, detailed morphological information is needed regarding the maxillae and the palatine bones, with greater and lesser palatine arteries running through the greater and lesser palatine canals and where communication with the nasopalatine artery from the incisive canal occurs. We investigated the morphology of the elderly cadaver palatine using CBCT and macroscopic observations. These observations provide useful information for dental clinic and implant treatments in the maxillary region.

## Methods

### Subjects

A total of 72 Japanese donor cadavers (48 female and 24 male cadavers, each donating either the left or right side of the maxilla; 59–94 years old; 49 dentate, 23 edentate) preserved in the Department of Anatomy of Nippon Dental University were used in this study. Using forceps, we removed the entire mucous membrane and the connective tissues of the palatine under macroscopic view using a stereomicroscope (Leica MZ 16; Leica Microsystems, USA) with Leica Application Suite software (Leica Microsystems, USA). We clearly identified the course of communication of the palatine artery, the ascending pharyngeal artery, the greater palatine nerve, the lesser palatine nerve, the nasopalatine nerve, the branch of the maxillary nerve, the vagus nerve and the glossopharyngeal nerve. In the dry skulls of the same Japanese donor cadavers, we also observed the morphological structure of the bony groove.

### CBCT scanning

For each serial CBCT image, we analyzed a cross-section at the center level of the maxillary first molar (AZ 3000CT; Asahi Roentgen Industry, Kyoto, Japan). CBCT (PSR 9000N; Asahi Roentgen Industry, Kyoto, Japan) was used in this study. Images of the incisive canal and surrounding structures were acquired for the samples. The CBCT machine was operated at a tube potential of 80 kV and a tube current of 4 mA, and the scans acquired cylindrical areas of 41 × 40 mm with high resolution (voxel size = 0.1 mm). From the three-dimensional CBCT images, the diameter of the skull was measured using ASAHI vision software (Asahi Roentgen Industry, Kyoto, Japan) and Micro AVS version 11 software (KGT Industry, Tokyo, Japan). After identifying the median sagittal plane and the palatal plane, images

were defined by the anterior and posterior nasal spines that were perpendicular to the median sagittal planes, as a reference plane. The measurement points in the palatine bony structures were as follows: incisive canal length (ICL), maximum incisive canal width of the nasal side (ICNW), maximum incisive canal width of the middle region of the canal (ICMW), maximum incisive canal width of the oral side (IOCW), palatine canal length (PCL), maximum palatine canal width of the pterygopalatine fossa side (PCPW), maximum palatine canal width of the middle region of the canal (PCMW), maximum palatine canal width of the greater foramen of the oral side (GPCW) and maximum palatine canal width of the lesser foramen of the oral side (LPCW) (see Fig. 1). We defined three groove structures: shallow groove, with a depth ranging from 1.5 to 3 mm; deep groove, with a depth > 3 mm; and flat groove, with a depth < 1.5 mm.

These measurements were performed by two hospital-based radiologists (R.A. & T.K.) who had a specialty training followed by a 10-year period of additional training in CBCT. All operators were based in their own department of Oral and Maxillofacial Radiology, School of Life Dentistry at Tokyo, The Nippon Dental University. Each measurement is one of three, from which the largest and smallest values were omitted.

### Statistical methods

The measurement data were analyzed using Student's *t* test/linear regression. Pearson's correlation coefficient was used to determine the correlations. The level of significance was set as  $p < 0.05$ . Results are reported as the mean ± SD. Statistical analyses were performed using IBM SPSS Statistics Base, version 22 (IBM, NY, USA).

## Results

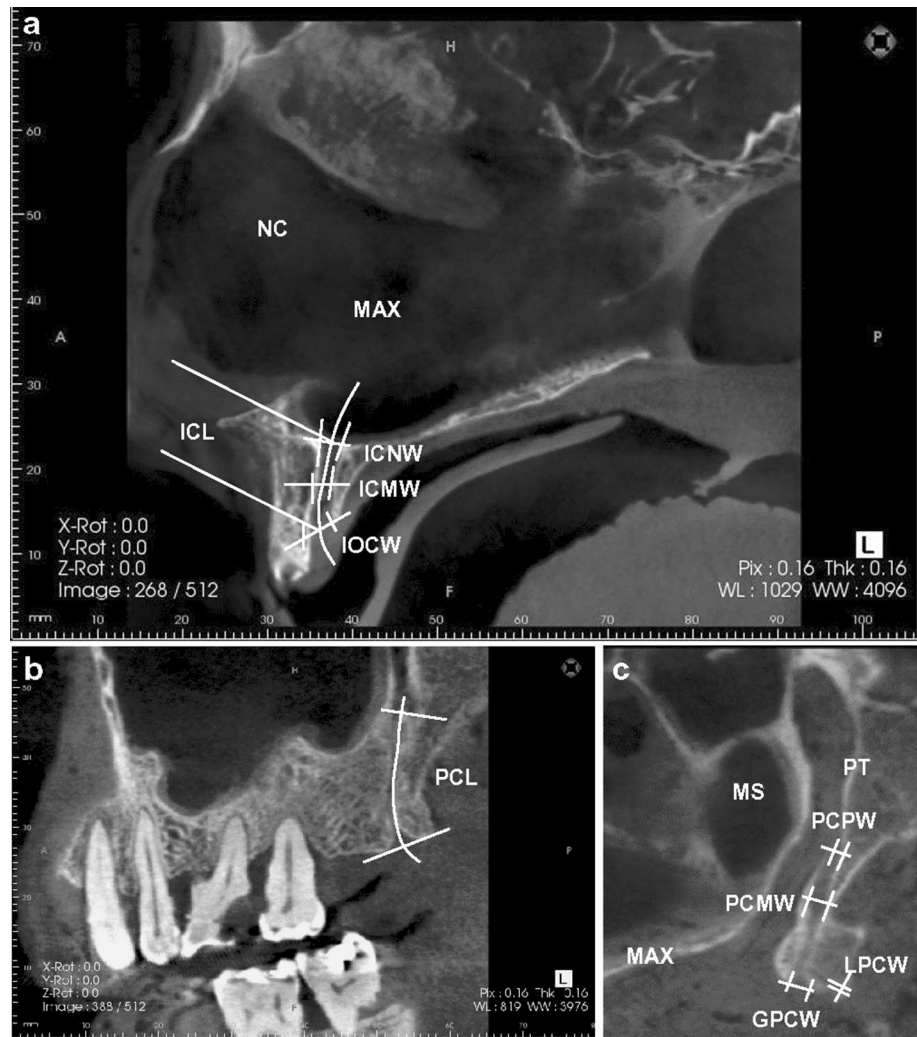
### CT images of the palatine

In the molar tooth region of the palatine process, the blood vessel and a nerve were identified in CBCT views in a bony groove. This tendency was remarkable in edentulous samples. The absence of a tooth causes the bony socket to form a palatine bony process.

We found three types of bony structures with the nerve root and the vessel from the greater palatine in the palatine process in the molar regions of the palatine: shallow groove (dentate: 20.4%, 20/98; edentulous: 34.8%, 16/46), deep groove (dentate: 48.0%, 47/98; edentulous: 50.0%, 23/46), and flat groove (dentate: 31.6%, 31/98; edentulous: 15.2%, 7/46) (Fig. 2). The deep groove structure was the most frequent in the examined maxillary specimens. In the molar

**Fig. 1** Measurement points in the palatine bony structure view in a sagittal section of a CBCT image of the human maxilla.

**a** Measurement points in the median sagittal plane are shown as follows: incisive canal length (ICL), maximum incisive canal width of the nasal side (ICNW), maximum incisive canal width of the middle region of the canal (ICMW), and maximum incisive canal width of the oral side (IOCW). **b** Palatine canal length (PCL) of the sagittal section of the maxilla. **c** Maximum palatine canal with greater foramen on the oral side, showing the maximum palatine canal width of the pterygopalatine fossa side (PCPW), maximum palatine canal width of the middle region of the canal (PCMW), maximum palatine canal width of the lesser foramen of the oral side (LPCW) and maximum palatine canal width of the greater foramen of the oral side (GPCW). *MAX* maxilla, *MS* maxillary sinus, *NC* nasal cavity, *PT* palatine



tooth region of the bony palatine process, the blood vessel and a nerve exist in CBCT views in a bony groove. This tendency is remarkable in an edentulous samples. The disappearance of the tooth causes the socket to form a palatine bony process.

### Properties of CBCT measurements of the palatal canal, incisive canal, greater palatine foramen, lesser palatine foramen and incisive foramen

We measured structures of the palatine bone at nine points as follows: ICL, ICNW, ICMW, IOCW, PCL, PCPW, PCMW, LPCW, and GPCW (see Fig. 1). However, gender, laterality, and dentulous and edentulous sample differences were observed in these measurements. We divided the data into the following two groups: (1) lesser palatal foramen smaller than 0.5 cm and (2) lesser palatal foramen larger than 0.5 cm. Significant differences were found in the PCL ( $p < 0.05$ ), GPCW ( $p < 0.05$ ), PCMW ( $p < 0.05$ ) and LPCW ( $< 0.5$  or  $\geq 0.5$  mm) groups. We also divided the

measurement data according to group size using the above-mentioned parameter: (1) GPCW smaller than 1.5 cm and (2) GPCW larger than 1.5 cm. Significant differences were also found in the PCPW ( $p < 0.05$ ) of the LPCW ( $< 1.5$  or  $\geq 1.5$  mm) groups (Table 1).

### Macroscopic observations (Figs. 3, 4, 5)

We observed the branches of the facial artery, the descending palatine artery and the ascending pharyngeal artery. These branches communicate with each other in two regions of the palatine: the soft palate and incisive region anastomosis. The branches of the facial artery include the ascending palatine artery. This artery ascends beneath the posterior belly of the digastric muscle. The branch of the maxillary artery is the descending palatine artery that runs downwards and supplies the mucous membrane of the roof of the mouth. Several small rami branches pass through the accessory palatine canals and supply the soft palate. The greater palatine artery is a continuation of the palatine that ascends through

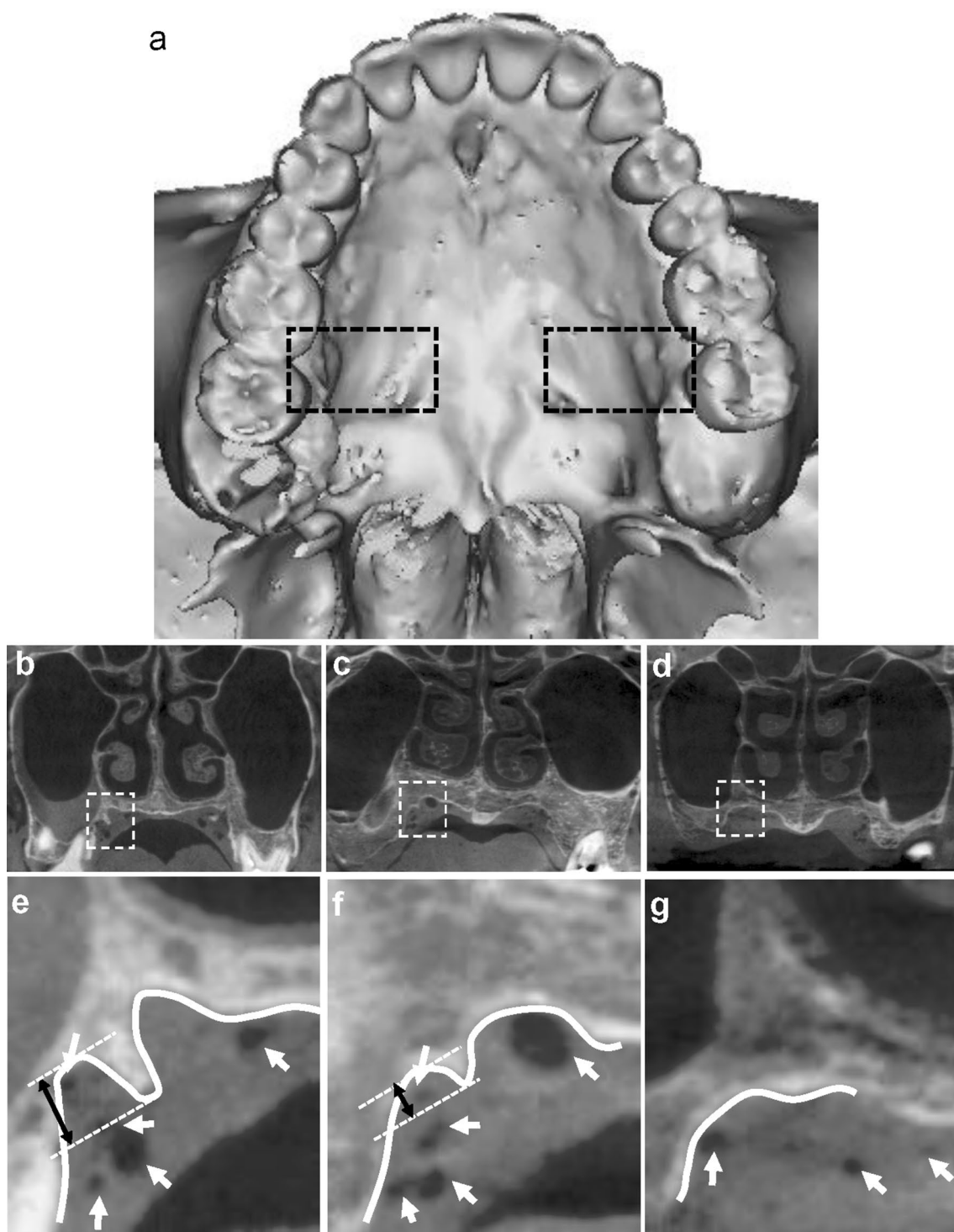


**Fig. 2** Three types of bony structures in the molar region of the palatine bones: shallow groove, deep groove, and flat groove. **a** 3D image of the palatal surface of the human skull. **b** Deep groove structure of the palatine in the frontal section of a human skull. The dotted-line square is a frontal section enlarged in **e**. **c** Shallow groove structure of the palatine in the frontal section of a human skull. The dotted-line square is a frontal section enlarged in **f**. **d** Flat groove structure of the palatine in the frontal section of a human skull. The dotted-line

square is a frontal section enlarged in **g**. **e** Large magnification of **b** shows as a schematic line structure of a deep groove type (see white line and dot lines). **f** Large magnification of **c** shows as a schematic line structure of a shallow groove (see white line). **g** Large magnification of **d** shows as a schematic line structure of a shallow groove (see white line). Black dotted line shows the frontal sections in **b–d**. Black arrow shows the depth of a bony groove. White dotted line shows the border of a bony groove. White arrows show the vessel lumen

**Table 1** The measurement data of each bony point

	ICL	IOCW	ICMW	ICNW	PCL	GPCW	LPCW	PCMW	PCPW
LPCW < 0.5	12.47 ± 3.45	4.04 ± 1.47	1.84 ± 1.28	3.18 ± 1.36	12.7 ± 3.01	1.02 ± 0.45	0.26 ± 0.009	0.58 ± 0.32	0.81 ± 0.45
LPCW ≥ 0.5	13.82 ± 3.0	5.08 ± 1.39	2.25 ± 1.27	3.40 ± 1.91	16.54 ± 3.19	1.71 ± 0.67	0.81 ± 0.28	1.15 ± 0.57	1.31 ± 1.06
GPCW < 1.5	12.35 ± 3.58	4.16 ± 1.69	1.72 ± 1.21	3.00 ± 1.54	12.8 ± 3.26	0.93 ± 0.36	0.4 ± 0.34	0.64 ± 0.32	0.75 ± 0.62
GPCW ≥ 1.5	14.18 ± 2.4	4.94 ± 1.38	2.52 ± 1.27	3.76 ± 1.54	16.52 ± 2.93	1.95 ± 0.49	0.56 ± 0.25	1.07 ± 0.68	1.47 ± 0.79

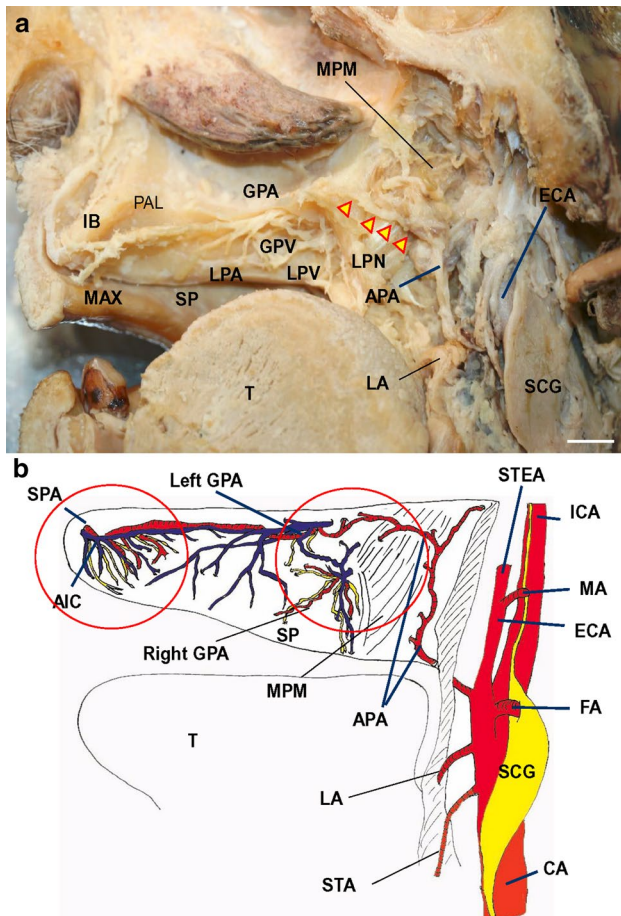


**Fig. 3** Macroscopic view of the inner surface of a sagittal section of a human head (86-year-old male). The pharyngeal artery runs through the inner side of the ascending medial pterygoid muscle and communicates with the greater palatine artery. The branch of the maxillary artery, such as the greater palatine artery, passes through the palatine canals and supplies the soft palate. The greater palatine artery communicates with the branch of the posterior lateral nasal artery (incisive region anastomosis) (a, b). b is a schema of a. Macroscopic view of anastomosis between the lesser palatine artery and the ascending pharyngeal artery and anastomosis between the incisive branch and the greater palatine artery. APA ascending pharyngeal artery, CA carotid artery, ECA external carotid artery, GPA greater palatine artery, GPV greater palatine vein, LA lingual artery, FA facial artery, IB incisor branch, ICA internal carotid artery, LPA lesser palatine artery, LPV lesser palatine vein, LPN lesser palatine nerve, MPM medial pterygoid muscle, MA maxillary artery, MAX maxilla, PAL palatine, SCG superior cervical ganglion, SPA sphenopalatine artery, STA superior thyroid artery, STEA superficial temporal artery, SP soft palate, T tongue. Bar = 10 mm

the incisive foramen and communicates with the posterior artery of the septum nasi (incisive region anastomosis). The communication of the ascending pharyngeal artery with the greater and lesser palatine arteries descends into the soft palate and the levator veli palatini muscle (soft palate anastomosis). We also observed that the bundle of nerves from the greater palatine and lesser palatine passes through the palatine canal and includes the nasopalatine nerve, a branch of the maxillary nerve, the vagus nerve and the glossopharyngeal nerve in the same region in which the artery passes through the palatine (Fig. 3). In our detailed observation, we defined a specific arrangement of the nerve and arteries in the molar region of the palatine. The greater palatine artery mainly runs medially, in contrast to the greater palatine nerve, which mainly runs on the buccal side through the great palatine foramen in dentate samples (Fig. 4). In contrast, the greater palatine artery, vein and nerve have almost no regular arrangement on the palatine side from the greater palatine foramen in edentulous samples (Fig. 5). The distribution of blood vessels and nerves becomes remarkable, and the lateral branches from the center to the buccal side increase from the molar area to the premolar area of the palatine. This tendency was remarkable in the dentate cases in our results. The divergence of the blood vessel and nerve becomes simple; lateral branches from the center to the buccal side and middle region increase from the molar area to the premolar area. This tendency was also remarkable in edentulous cases (Figs. 4, 5).

## Discussion

Morphological observation of the palatine provides useful data for assisting periodontists in planning dimensions and harvesting connective tissue grafts from the palate [13]. In general, harvesting from the palatine is performed in particular neighboring areas in which there is sufficient bone quantity, with minimal autogenous bone needed for palatal flap surgery [5]. A more detailed understanding of the arrangement of blood vessels and nerves is needed to decide whether to harvest bone and connective tissue from an area. In our macroscopic results, two structural properties and the arrangement of nerves and blood vessels were identified: incisive region anastomosis and soft palate anastomosis in

**Fig. 4** Macroscopic inner surface of a sagittal view of both sides of a dentate case in a human head. In the molar region of the palatine, the greater palatine artery runs on the middle side, and the greater palatine nerve runs on the buccal side through the palatine canal. The arrangement of these arteries and nerves on the palatine process of the maxillae is complex. **a** Right side of the human head; **b** left side of the human head (73-year-old female). *GPA* greater palatine artery, *GPV* greater palatine vein, *GPN* greater palatine nerve, *LPA* lesser palatine artery, *LPV* lesser palatine vein, *LPN* lesser palatine nerve, *PAL* palatine, *PPM* palatopharyngeal membrane. Bar = 10 mm

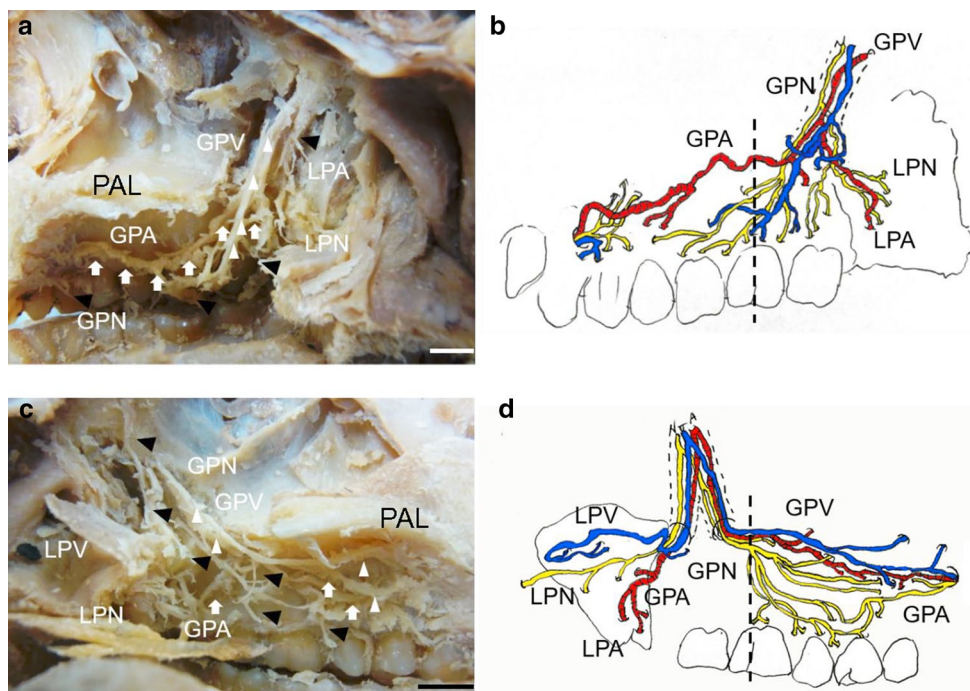
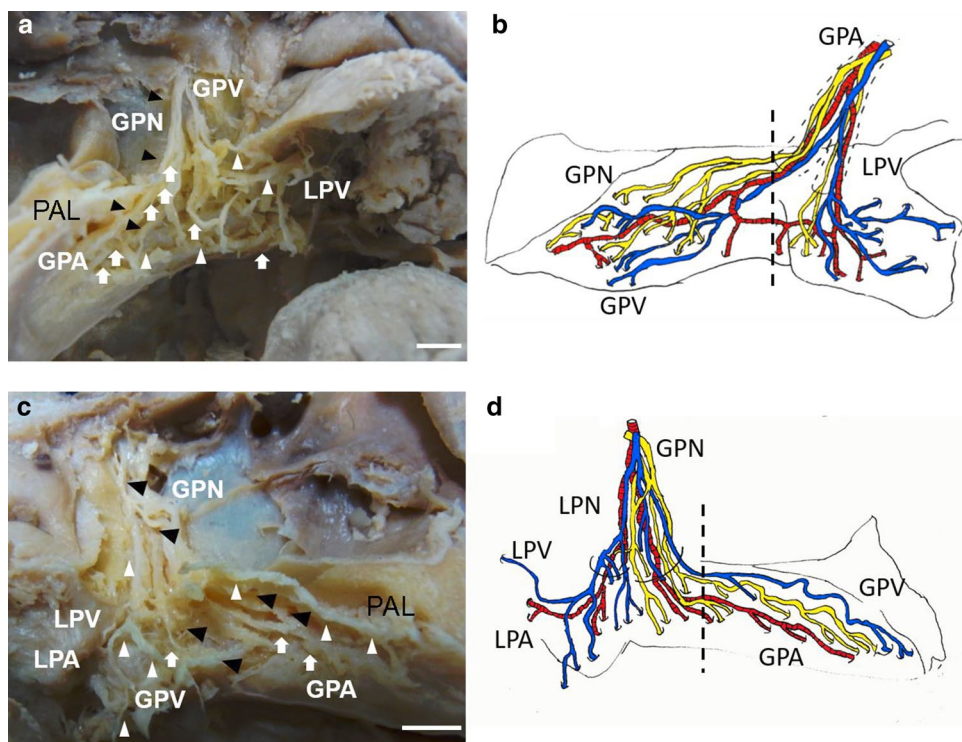


**Fig. 5** Macroscopic inner surface of a sagittal view of both sides of an edentulous case in a human head. In the molar region of the palatine, the greater palatine arteries and nerves were found in the palatine process of the maxilla. However, the greater palatine artery, vein and nerve have almost no regular arrangement running on the palatine side through the palatine canal in edentulous samples. **a** Right side of the human head; **b** left side of the human head (85-year-old male). *GPA* greater palatine artery, *GPV* greater palatine vein, *GPN* greater palatine nerve, *LPA* lesser palatine artery, *LPV* lesser palatine vein, *LPN* lesser palatine nerve, *PAL* palatine, *PPM* palatopharyngeal membrane. Bar = 10 mm



the palatine area. Moreover, the specific complex arrangement of blood vessels and nerves in the two regions differed in dentate and edentulous samples. The greater palatine artery mainly runs medially, and the greater palatine nerve runs on the buccal side through the greater palatine foramen, which is in contrast to edentulous samples. Klosek and

Rungruang [13] reported that measurements from the incisor foramen to the nasal spine of the greater palatine artery branch differed according to gender; most of the branches were observed on the alveolar process side of the maxilla. However, our data do not consider gender because different measurement points were obtained for the greater and lesser

palatine foramina regions. Moreover, significant differences in the size of the lesser palatine were found in the PCL ( $p < 0.05$ ), the GPCW ( $p < 0.05$ ), and the PCMW ( $p < 0.05$ ). The palatine canal and greater palatine foramen depend on the location and size of the lesser palatine foramen. Therefore, the lesser palatine foramen may be one of the key palatine components. The different distributions of blood vessels provide useful information for avoiding infection in the donor side from autogenous bone harvesting between dentate and edentulous maxillae. Therefore, we need to consider the morphological characteristics of the palatine canal in dental clinics and during implant treatments. However, CBCT analysis of various conditions causing loss of teeth in dentate and edentulous samples in donor cadavers is needed.

Therefore, morphological information about the maxillae and the palatine bones will provide useful information for dental clinic and implant treatments in the maxillary region.

### **Anatomical features of blood vessels and nerves in the distribution of the bone in the palatine**

Maxillary blood vessel and nerve paths have morphologically more difficult macroscopic features than those in the mandible. There is no mucosal lamina propria in the palatine, so blood vessels and nerves travel in the narrow spaces of the human palatine. Moreover, the vessels and nerves of the palatine mainly run through bony grooves near the greater and lesser palatine foramina. In our results, these blood vessels and the nerves of the palatine ran remarkably close to the molar and premolar areas of the bony palatine canals in edentulous samples. Many side branches enter from the middle of the tooth root, in addition to nerves and blood vessels entering from the apex of the root. Incomplete longitudinal palatine grooves and canals and one-groove bordered areas, e.g., with bony ridges, were found in the premolar and molar regions of the palatine with blood vessels and nerves. Such bridges were also typically found in the posterior portion of the canal [26]. Moreover, Ozcan et al. [17] reported that the palatal root of the maxillary molar was found to be the longest and that of the disto-buccal root the shortest. The length of the disto-buccal root canal of the maxillary molars was the shortest. The maxillary molars exhibited more one-canal than two-canal roots in the posterior region of the palatine process. An elongated palatal root is required to maintain the bony structure of the maxillae. Therefore, the palatal root of the maxillary molar roots may affect the location and course of the bony canal passing the greater palatine artery and nerve as well as affect the structures of alveolar bone in the premolar and molar regions of the maxilla. Moreover, many previous reports indicated the location of the greater palatine foramen to be in the molar region. The greater palatine foramen opened antero-medially in 74% of specimens examined. In Ajmani [2], the most common position of the foramen was

found to be medial or opposite the third maxillary molar, and the direction of the foramen opening into the oral cavity was inferior in an anteromedial direction in 58.5% of Nigerian and 91.1% of Indian skulls. Sujatha et al. [22] indicated that the most common location of the foramen was opposite the third molar (86.0%). The greater palatine was mainly found at the third maxillary molar in previous reports [6, 8, 19, 24]. In our results, the greater palatine foramen was mainly located at the third maxillary molar in edentulous cases. The bony canal and maxillary groove were mainly found in dentate cases. These bony canals and grooves contained palatine nerves and vessels running unilaterally, and these bony structures may affect the risk associated with peripherally blocking the maxillary nerve during maxillo-facial surgery. Wong and Sved [25] indicated the value of anesthetizing the maxillary nerve with local anesthesia, and the extractions performed in patients required a general anesthetic. Harnet et al. [10] suggested that the vessels and nerve are directly related to the pterygopalatine segment of the maxillary artery and nerve. Our CBCT study demonstrating this bony canal allows for a better understanding and the accomplishment of surgical or anesthetic treatments. Hafeez et al. [9] also indicated that the intra-canalicular branching variations of the greater palatine nerve provided useful information for possible implications in clinical practice. Aoun et al. [3] indicated that a maxillary nerve block through the greater palatine canal is rarely adopted by dental practitioners because of a lack of experience in the technique, which may lead to several complications. Moreover, the distribution of blood vessels and nerves becomes remarkable, and the lateral branches from the center to the buccal side increase from the molar area to the premolar area of the palatine. This tendency is remarkable in the dentate cases in our study. The divergence of the blood vessels and nerves becomes simple, and lateral branches from the center to the buccal side and middle region increase from the molar area to the premolar area. This tendency is also remarkable in the edentulous cases in our study. In general, branches of the inferior alveolar nerve and artery remain in the canals and travel through the maxilla during the resorption of alveolar bone. The evidence of bone resorption and the lack of alveolar bone occurred in the complex remodeling process as a result of tooth bud resorption. Therefore, morphological information about the maxillae and the palatine bones will provide useful information for dental clinic and implant treatments in the maxillary region.

### **Conclusions**

More detailed morphological information is needed for the maxillae and the palatine bones with greater and lesser palatine arteries and nerves for improved dental care and implant treatments in the maxillary region. We investigated the morphology of the elderly cadaver palatine using CBCT

and macroscopic observations. The lesser palatine canal structure may be affected differently in edentulous maxillae than in dentate maxillae. Differences in the supply of the greater and lesser palatine arteries and nerves were identified between edentulous and dentate maxilla. These observations will provide useful information for dental care and implant treatments for oral conditions in the maxillary region.

**Author contributions** Protocol/project development: IS, YM. Data collection and management: RA, TK. Data analysis: YM, YM. Manuscript writing/editing IS, YM.

## Compliance with ethical standards

**Conflict of interest** The authors declare that they have no conflict of interest.

## References

1. Agur AM, Dalley AF (2009) Grant's atlas of anatomy. Lippincott Williams & Wilkins, Philadelphia
2. Ajmani ML (1994) Anatomical variation in position of the greater palatine foramen in the adult human skull. *J Anat* 184:635–637
3. Aoun G, Zaarour I, Sokhn S, Nasseh I (2015) Maxillary nerve block via the greater palatine canal: an old technique revisited. *J Int Soc Prev Community Dent* 5:359–364. <https://doi.org/10.4103/2231-0762.165930>
4. Bornstein MM, Lauber R, Sendi P, von Arx T (2011) Comparison of periapical radiography and limited cone-beam computed tomography in mandibular molars for analysis of anatomical landmarks before apical surgery. *J Endod* 37:151–157. <https://doi.org/10.1016/j.joen>
5. Cagimni P, Govsa F, Ozer MA, Kazak Z (2017) Computerized analysis of the greater palatine foramen to gain the palatine neurovascular bundle during palatal surgery. *Surg Radiol Anat* 39:177–184. <https://doi.org/10.1007/s00276-016-1691-0>
6. Chrcanovic BR, Custódio AL (2011) Optic, oculomotor, abducens, and facial nerve palsies after combined maxillary and mandibular osteotomy: case report. *J Oral Maxillofac Surg* 69:e234–e241. <https://doi.org/10.1016/j.joms.2011.01.001>
7. El Nahass H, Naiem SN (2015) Analysis of the dimensions of the labial bone wall in the anterior maxilla: a cone-beam computed tomography study. *Clin Oral Implants Res* 26:e57–e61. <https://doi.org/10.1111/clr.12332>
8. Gibelli D, Borlando A, Dolci C, Pucciarelli V, Cattaneo C, Sforza C (2017) Anatomical characteristics of greater palatine foramen: a novel point of view. *Surg Radiol Anat*. <https://doi.org/10.1007/s00276-017-1899-7>
9. Hafeez NS, Ganapathy S, Sondekoppam R, Johnson M, Merrifield P, Galil KA (2015) Anatomical variation of the greater palatine nerve in the greater palatine canal. *J Can Dent Assoc* 81:f14
10. Harnet JC, Feki A, Maillot C (1994) The greater palatine canal. Radio-anatomical study and clinical value. *J Radiol* 75:287–293
11. Hochstetter F (1948) *Toldts Anatomischer Atlas, Band 1*, Wien, Urban & Schwarzenberg, 21 Auflage
12. Jeyaseelan N, Gupta M (1988) Canals for the greater palatine nerve and vessels in the hard palate. *J Anat* 156:231–233
13. Klosek SK, Rungruang T (2009) Anatomical study of the greater palatine artery and related structures of the palatal vault: considerations for palate as the subepithelial connective tissue graft donor site. *Surg Radiol Anat* 31:245–250. <https://doi.org/10.1007/s00276-008-0432-4>
14. Kopsch F (1922) *Lehrbuch und Atlas der Anatomie des Menschen*. Georg Thieme, Leipzig, pp 294–325
15. Monnet-Corti V, Santini A, Glise JM, Fouque-Deruelle C, Dillier FL, Liébart MF, Borghetti A (2006) Connective tissue graft for gingival recession treatment: assessment of the maximum graft dimensions at the palatal vault as a donor site. *J Periodontol* 77:899–902
16. Nishi S (1974) *Topographical atlas of human anatomy*. Kanehara Shuppan, Tokyo
17. Ozcan G, Sekerci AE, Cantekin K, Aydinbelge M, Dogan S (2016) Evaluation of root canal morphology of human primary molars by using CBCT and comprehensive review of the literature. *Acta Odontol Scand* 74:250–258. <https://doi.org/10.3109/00016357>
18. Pandharbale AA, Gadgil RM, Bhoosreddy AR, Kunte VR, Ahire BS, Shinde MR, Joshi SS (2016) Evaluation of the posterior superior alveolar artery using cone beam computed tomography. *Pol J Radiol* 19:606–610. <https://doi.org/10.4317/jced.53213>
19. Piagkou M, Xanthos T, Anagnostopoulou S, Demesticha T, Kotsiomitris E, Piagkos G, Protogerou V, Lappas D, Skandalakis P, Johnson EO (2012) Anatomical variation and morphology in the position of the palatine foramina in adult human skulls from Greece. *J Craniomaxillofac Surg* 40:e206–e210. <https://doi.org/10.1016/j.jcms.2011.10.011>
20. Sato I, Kawai T, Yoshida S, Miwa Y, Imura K, Asaumi R, Sunohara M, Yosue T (2010) Observing the bony canal structure of the human maxillary sinus in Japanese cadavers using cone beam CT. *Okajimas Folia Anat Jpn* 87:123–128
21. Spalteholz W (1939) *Hand Atlas der Anatomie des Menschen, Band 1*, Leipzig, 14 Auflage
22. Sujatha N, Manjunath KY, Balasubramanyam V (2005) Variations of the location of the greater palatine foramina in dry human skulls. *Indian J Dent Res* 16:99–102
23. Taylor TD (ed) (2000) *Clinical maxillofacial prosthetics*. Quintessence Publishing Co Inc., Chicago, pp 155–170
24. Tomaszewska IM, Kmiotek EK, Pena IZ, Średniawa M, Czyżowska K, Chrzan R, Nowakowski M, Walocha JA (2014) Computed tomography morphometric analysis of the greater palatine canal: a study of 1500 head CT scans and a systematic review of literature. *Anat Sci Int* 2015 90:287–297. <https://doi.org/10.1007/s12565-014-0263-9>
25. Wong JD, Sved AM (1991) Wong via the greater palatine canal: a modified technique and case reports. *Aust Dent J* 36:15–21
26. Zivanović S (1980) Longitudinal grooves and canals of the human hard palate. *Anat Anz* 147:161–167